

AMORPHOUS SILICON PASSIVATION APPLIED TO THE FRONT SIDE BORON EMITTER OF *n*-TYPE SILICON SOLAR CELLS

A. Richter, J. Benick, M. Hermle and S.W. Glunz

Fraunhofer Institute for Solar Energy Systems (ISE), Heidenhofstrasse 2, D-79110 Freiburg, Germany

Phone +49-761-4588-5395; Fax +49-761-4588-9250; Email: Armin.Richter@ise.fraunhofer.de

ABSTRACT: Hydrogenated amorphous silicon (*a*-Si:H) was used to passivate the front side boron emitter of *n*-type silicon solar cells. The main aspect was to investigate the parasitic absorption behavior of the *a*-Si:H layers on the solar cells front side with different thicknesses between 5 nm and 20 nm. Therefore planar solar cells featuring a diffused boron emitter and a diffused back surface field were fabricated. The cells reached energy conversion efficiencies up to 17.8% with an open-circuit voltage V_{OC} of 641 mV for an *a*-Si:H thickness of 15 nm. Analogous processed reference cells, with an Al₂O₃ passivated emitter achieved an efficiency of 19% and a V_{OC} of 658 mV.

Keywords: *a*-Si, passivation, emitter, *n*-type solar cells

1 INTRODUCTION

Recently, there has been an increasing interest in *n*-type crystalline silicon in the field of silicon solar cell research. This is mainly related to two main physical advantages. First, *n*-type silicon shows a higher tolerance to common impurities (e.g. Fe) compared to *p*-type silicon [1]. And second, *n*-type silicon does not suffer from the boron-oxygen related light-induced degradation (LID), which is known for solar cells based on *p*-type Czochralski silicon [2]. However, an effective passivation of the front side boron emitter is a prerequisite to profit from the high material quality of *n*-type silicon. Unfortunately, common passivation layers for the passivation of highly phosphorus doped surfaces (e.g. SiN_x, SiO₂) do not show a comparable performance on highly boron doped surfaces [3]. Thus alternative layers for the passivation of *p*⁺-type surfaces have to be developed. One promising candidate for the passivation of highly boron doped surfaces is Al₂O₃, which already has been applied successfully as surface passivation layer on high efficiency *n*-type PERL solar cells [4, 5]. Nevertheless, the deposition technique that has been applied for the deposition of the Al₂O₃ – plasma assisted atomic layer deposition (ALD) – is relatively slow, and thus might not be appropriate to meet the high throughput demands of the photovoltaic industry.

Alternatively the front side boron emitter can be passivated by hydrogenated amorphous silicon (*a*-Si:H). *a*-Si:H also shows an excellent passivation quality on highly doped boron emitters [3], as well as on *n*-type and *p*-type *c*-Si [6]. These *a*-Si:H layers are deposited by plasma enhanced chemical vapor deposition (PECVD) at low temperatures below 260 °C. Together with the COSIMA technique [7], where the *a*-Si:H is dissolved in the overlaying aluminum by annealing at around 260 °C, a simple low temperature process sequence for the realization of the solar cell front side exists. However, due to the absorption of *a*-Si:H in the uv-vis range, the *a*-Si:H thickness needs to be limited to ultrathin layers. For *a*-Si:H thicknesses above 10 nm, Plagwitz *et al.* [8] observed a strong decrease of the internal quantum efficiency *IQE* as well as in the short circuit current density J_{SC} on *n*⁺*p* solar cells. A reduction of the layer thickness below about 7 nm was attended by a decrease in the passivation quality. Thus, regarding the efficiency of solar cells, there should be an optimum layer thickness featur-

ing a sufficient surface passivation quality with a minimum of parasitic absorption losses.

In the present work we applied *a*-Si:H of varying layer thicknesses as passivation of the front side boron emitter of *n*-type silicon solar cells. This work is focused on the investigation of the absorption behavior of the ultrathin *a*-Si:H layers. Therefore we decided to fabricate rather simple solar cells with a planar surface and a phosphorous back surface field (BSF).

2 EXPERIMENTAL

To study the impact of the *a*-Si:H layer thickness on the passivation quality at boron emitters, symmetrical *p*⁺*np*⁺ lifetime samples were fabricated on shiny-etched (100)-orientated 1 Ωcm *n*-type float-zone (FZ) silicon wafers with a thickness of 250 μm. The thickness of the *a*-Si:H layer was varied between 5 and 20 nm. To be comparable to the solar cell front side, the *a*-Si:H layers are covered by a 60 nm thick SiN_x antireflection coating. The structure of the *p*⁺*np*⁺ lifetime samples is schematically shown in Figure 1a. In addition to the *p*⁺*np*⁺ samples, reference lifetime samples on lowly doped *p*-type substrates have been prepared with flat (100)-orientated 1 Ω cm *p*-type FZ-Si wafers.

A tube furnace with BBr₃ as diffusion source was used for the emitter formation. After the removal of the boron glass by etching in a buffered HF-solution, a drive-in diffusion in an argon atmosphere was performed. Subsequently, the emitters received an additional “drive-in diffusion” by a thermal oxidation process. Different oxidation processes resulting in a 30 nm and a 105 nm thick oxide were applied. After the drive-in the oxides were removed again. The surface doping concentration of the respective emitters are 1×10¹⁹ cm⁻³ and 6×10¹⁸ cm⁻³ (see figure 2). In the following, these emitters are referred to as shallow and deep emitter, respectively.

A direct parallel plate PECVD reactor, operated at a plasma excitation frequency of 13.56 MHz, was used for the deposition of *a*-Si:H as well as SiN_x. The deposition of both layers was performed at a temperature of 250 °C. The effective minority carrier lifetime was determined from quasi-steady-state photoconductance (QSSPC) measurements [9]. The layer thickness as well as the optical constants of the *a*-Si:H and the SiN_x layers were

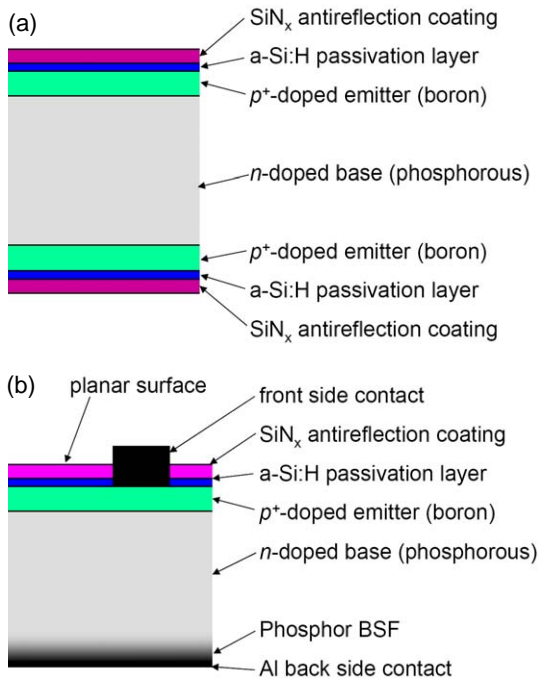


Figure 1: Schematic structure of the symmetrical p^+np^+ -lifetime samples (a) and the solar cells (b) investigated in this work. The solar cells feature a planar front side which is passivated with the same $a\text{-Si:H/SiN}_x$ layer stack as the p^+np^+ -lifetime samples. The back side is passivated by a phosphorous doped BSF.

measured using a spectroscopic ellipsometer (J. A. Woolam) and the data analysis method according to Ref. [10].

For the investigations on n -type silicon solar cells, $2 \times 2 \text{ cm}^2$ solar cells with a planar surface and $a\text{-Si:H}$ layer thicknesses between 5 and 20 nm were fabricated. Figure 1b shows the structure of the solar cells schematically. The same substrate as for the p^+np^+ lifetime samples (shiny-etched (100)-orientated $1 \Omega\text{cm}$ n -type FZ-Si, thickness 250 μm , 4" diameter) was used for the solar cells. Seven solar cells were placed on each wafer. The back side of the solar cells was passivated by a Gaussian-shaped 3 μm deep phosphorous diffused (POCl_3) BSF with a surface doping concentration of $5 \times 10^{19} \text{ cm}^{-3}$. The BSF was contacted on the whole area by evaporated aluminum. On the front side the boron emitter and its passivation by the $a\text{-Si:H/SiN}_x$ stack was processed analogous to the p^+np^+ lifetime samples whereas the deep emitter was applied. To realize the front side contacts, the SiN_x was locally opened by photolithography and the evaporated aluminum was structured by a lift-off process. Subsequently the COSIMA technique was applied to contact the emitter through the thin $a\text{-Si:H}$ layer.

For an accurate determination of the $a\text{-Si:H}$ layer thicknesses on the fabricated solar cells, these were measured before the solar cells were coated with SiN_x . The ideal SiN_x antireflection coating thickness for each $a\text{-Si:H}$ thickness was simulated by using the ray tracing simulation software SUNRAYS [11] and measured optical constants of $a\text{-Si:H}$ and SiN_x . The optical constants of $a\text{-Si:H}$ and SiN_x were determined on wafers, which were either coated by $a\text{-Si:H}$ or by SiN_x , but not by a stack

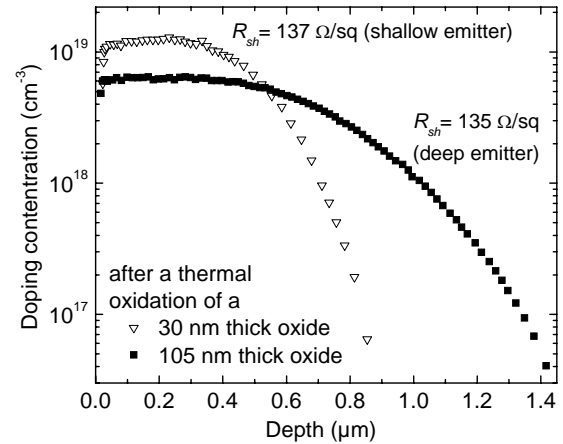


Figure 2: Measured boron doping profile after a drive-in diffusion process in Argon ambience and after an additional "drive-in" with a thermal oxidation of a 30 nm and a 105 nm thick oxide, respectively. The sheet resistances R_{sh} of both emitters is also given in the graph.

system of both to ensure a more reliable evaluation of the measured ellipsometric angles. The optimum SiN_x layer thickness for the planar solar cells varies between 70 nm for a 5 nm thick $a\text{-Si:H}$ layer and 76 nm for a 20 nm thick $a\text{-Si:H}$ layer.

For comparison, reference solar cells were fabricated analogous to the described p^+np^+ solar cells, which were passivated instead of the $a\text{-Si:H/SiN}_x$ stack by 30 nm Al_2O_3 covered by a 40 nm SiN_x antireflection coating. The Al_2O_3 layer was deposited by plasma-assisted ALD. In order to attain the passivating effect of Al_2O_3 , the cells were annealed at 425 $^\circ\text{C}$ for 25 minutes in forming gas ambience.

3 THICKNESS DEPENDENT PASSIVATION QUALITY

Figure 3 shows the passivation quality in terms of the measured effective lifetime τ_{eff} of the $a\text{-Si:H/SiN}_x$ passivated p^+np^+ lifetime samples (shallow emitter) as a function of $a\text{-Si:H}$ thickness. For comparison, the passivation quality achieved on the lowly doped surfaces of the p -type samples is also shown in the figure. All measured effective lifetimes are determined at an excess carrier density of $1 \times 10^{15} \text{ cm}^{-3}$.

It can be seen, that the p^+np^+ samples show the same $a\text{-Si:H}$ thickness dependence as the p -type samples. For a thickness of the $a\text{-Si:H}$ layer above 10 nm the passivation quality is independent of the actual layer thickness. For an $a\text{-Si:H}$ thickness below 8 nm however a strong decrease of the passivation quality can be observed.

The same trend, a reduced passivation quality for $a\text{-Si:H}$ layer thicknesses below around 8 nm, were also reported by other authors [8, 12]. Hence, for the application on solar cells, the optimum $a\text{-Si:H}$ layer thickness should be in the range of between 8 nm and 10 nm, where the passivation of the emitter is not affected by the $a\text{-Si:H}$ thickness, while the absorption losses within the $a\text{-Si:H}$ should be at a minimum.

4 SOLAR CELLS

An overview of the measured I - V parameters of the fabricated p^+nm^+ solar cells is given in Figure 4. The open-circuit voltage V_{OC} , the short-circuit current density J_{SC} and the energy conversion efficiency η are shown as a function of the a -Si:H layer thickness. For each a -Si:H thickness and I - V parameter, the average of the 7 solar cells per wafer is given as well as the value of the best cell. The error bars denote the standard deviation. In addition to the results of the a -Si:H passivated solar cells, the parameters of the Al_2O_3 passivated solar cells are also shown. All I - V parameters were obtained under an illumination at 1 sun AM1.5g.

As can be seen from Figure 4, the energy conversion efficiency achieved with the a -Si:H passivated p^+nm^+ solar cells is at an average level of $17.3 \pm 0.3\%$ for a -Si:H thicknesses above 5 nm. A maximum efficiency of 17.8% was achieved for a 15 nm thick a -Si:H passivation. The fill factors FF , which are not shown in detail, achieved a level of $80.2 \pm 1.1\%$ with a maximum of 81.6%, which proves the effective contact formation via the COSIMA technique. However, for the reference solar cells, where the boron emitter is passivated by Al_2O_3 , a significantly higher efficiency level of 19.0% could be reached. This is due to both a higher V_{OC} and a higher J_{SC} , which demonstrates that Al_2O_3 provides a superior passivation on highly boron doped surfaces. The achieved V_{OC} values of up to 657 mV is close to the maximum V_{OC} of ~ 665 mV that can be achieved with the applied full area BSF solar cell structure. That maximum V_{OC} level was simulated using PC1D [13] assuming an ideal front side passivation without surface recombination.

The passivation quality of the a -Si:H passivated solar cells in terms of the V_{OC} shows no clear dependence on the a -Si:H layer thickness. Instead of that, the V_{OC} seems to be very constant at a level of 637 ± 7 mV on average. Even if the a -Si:H thickness is below the critical value of ~ 10 nm, which was found for the lifetime samples, the

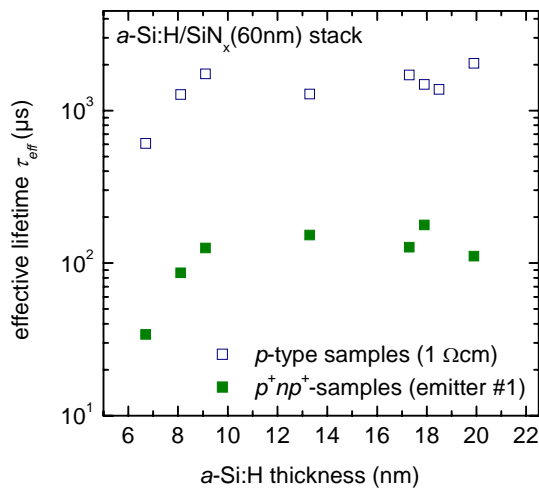


Figure 3: Measured effective minority carrier lifetimes τ_{eff} of the p^+np^+ samples featuring the shallow emitter (with a surface boron concentration of $1 \times 10^{19} \text{ cm}^{-3}$), as well as for the reference p -type samples. The effective lifetimes are given for an excess carrier density of $1 \times 10^{15} \text{ cm}^{-3}$.

solar cells show no clear decrease in the V_{OC} . Actually, the solar cells with a -Si:H thicknesses of 5 nm achieved the highest V_{OC} values of the a -Si:H passivated solar cells up to 647 mV. The high V_{OC} level of 658 mV of the Al_2O_3 passivated reference cells demonstrates the V_{OC} potential of the solar cells. Thus the V_{OC} level reached by the a -Si:H passivated solar cells is not limited by the recombination at the relative simple back side passivation with the phosphorous BSF.

The characteristic of the J_{SC} shows also no clear dependence on the a -Si:H thickness. Interestingly, only the cells passivated by the thinnest a -Si:H layer with a thickness of 5 nm show a reduced J_{SC} . Since those cells reached a V_{OC} up to 647 mV, the reduction of the J_{SC} can not be related to a reduced surface passivation, as would

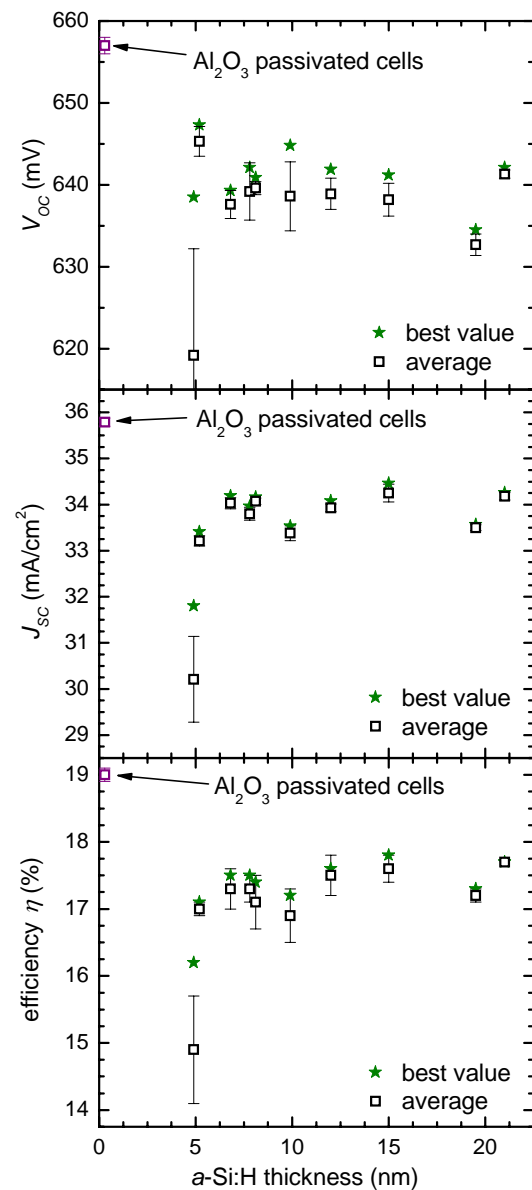


Figure 4: Open-circuit voltage V_{OC} , short-circuit current density J_{SC} and energy conversion efficiency η as a function of the a -Si:H layer thickness. The values are extracted from the measured I - V characteristic of the fabricated p^+nm^+ solar cells. Shown are the average of the seven cells per wafer and the value of the respective best cell.

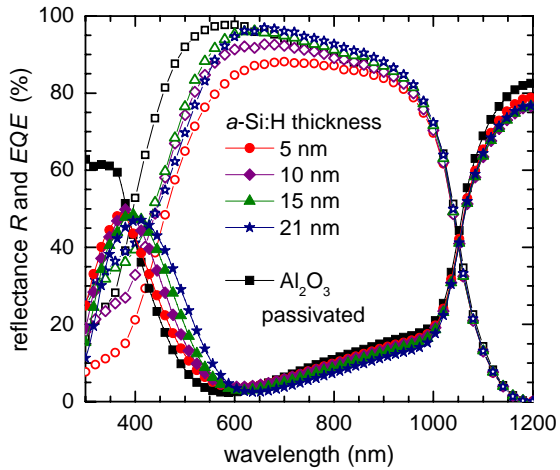


Figure 5: Measured reflectance spectra R (filled symbols) and external quantum efficiency EQE (open symbols) of the a -Si:H/ SiN_x passivated solar cells and a Al_2O_3 passivated reference cell.

be expected from the lifetime samples passivated with equivalently thin layers. The solar cells featuring a -Si:H thicknesses above 5 nm show a relatively constant J_{SC} level of $33.7 \pm 0.5 \text{ mA/cm}^2$ on average with a maximum of 34.5 mA/cm^2 at an a -Si:H thickness of 15 nm and an also rather high value of 34.3 mA/cm^2 for the cells passivated by an 21 nm thick a -Si:H layer. Due to the increasing absorption within the a -Si:H layer for an increasing thickness of a -Si:H, it would be expected that also the J_{SC} decreases with increasing a -Si:H thickness. To quantify the expected losses in the J_{SC} due to the absorption within the a -Si:H layer, the absolute absorption loss within the a -Si:H was simulated by SUNRAYS at an illumination of 1 sun (AM1.5g) as a function of the a -Si:H thickness for the optimized SiN_x thicknesses. The simulation was performed using measured optical constants for the applied a -Si:H and SiN_x . When increasing the a -Si:H layer thickness from 10 nm to 20 nm, the simulation results in an absolute loss of 1.4 mA/cm^2 . On a -Si:H passivated n^+p solar cells Plagwitz *et al.* observed a reduction in the J_{SC} from 33 mA/cm^2 to 31 mA/cm^2 for an increase in the a -Si:H thickness from 10 nm to 30 nm [8], which is in good agreement to our simulation calculations. However, such a decrease of the J_{SC} is not found for the p^+nn^+ solar cells fabricated within this work. However, the J_{SC} is affected by the red shift of the reflectance minima of the solar cells with an increasing a -Si:H thickness (see Figure 5). As mentioned above, we optimized the SiN_x thickness with respect to the a -Si:H thickness by optical simulations with SUNRAYS. These simulations yielded to an optimum SiN_x thickness of 70 nm for a 5 nm and 76 nm for a 20 nm thick a -Si:H layer, which shifts the minimum of the reflectance from 600 nm to 640 nm. Thus the cells with the thicker a -Si:H layers benefit from the reduced reflection in the long wavelength range, where a -Si:H is not absorbing. This can be clearly seen from the measured external quantum efficiency EQE in Figure 5.

To get a deeper insight into the optical and electrical effects that are originated by the front side a -Si:H layer, we calculated the internal quantum efficiencies IQE by means of the EQE and the reflectance. Since the absorption of the front a -Si:H/ SiN_x stack was neglected, this are

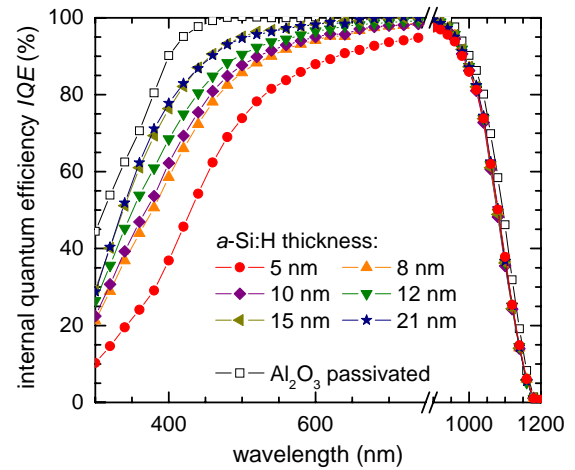


Figure 6: Measured internal quantum efficiency IQE of the fabricated p^+nn^+ solar cells, where the thickness of the a -Si:H passivation layer on top of front emitter was varied from 5 nm to 20 nm. The IQE of an Al_2O_3 passivated reference p^+nn^+ solar cells is also plotted.

included in the calculated IQE . The IQE was determined for several solar cells, which were passivated by a -Si:H layers of thicknesses between 5 nm and 21 nm. The optical band gap of hydrogenated amorphous silicon is in the range of 1.8 eV, which corresponds to a wavelength of about 690 nm. Since photons with an energy above 1.8 eV have a penetration depth in crystalline silicon below $5.8 \mu\text{m}$, the IQE in the wavelength range below 690 nm is sensitive on both, the emitter surface recombination and the parasitic absorption losses within the a -Si:H. If it is assumed that the absorption loss within the a -Si:H is approximately proportional to its thickness, which was found by the SUNRAYS simulations, and that the emitter surface recombination is approximately independent of the a -Si:H thickness, which corresponds to the thickness independent V_{OC} , it would be expected that the IQE in the short wavelength range decreases with an increasing thickness of the a -Si:H layer. However, exactly the opposite trend was observed for our a -Si:H passivated p^+nn^+ solar cells. From Figure 6 it can be seen, that an increasing thickness of the a -Si:H does not lead to a decrease in the IQE . On the contrary, the IQE increases with an increasing thickness of the a -Si:H. However, this behavior corresponds actually to an increasing passivation quality with increasing a -Si:H thickness, which is not reflected by an increasing V_{OC} with increasing a -Si:H thickness. The behavior of the IQE as a function of the a -Si:H thickness is not yet understood and further work has to be done to find an explanation for the observed behavior.

Another effect that can be observed is the – in general – relatively low level of the IQE in the short wavelength range, which does not really correspond to the relatively high V_{OC} level that have been measured for these solar cells. In particular, the reference solar cells passivated by Al_2O_3 also show a very low IQE in the short wavelength range, that can not be caused by recombinative losses as the measured V_{OC} of 658 mV is very close to the theoretical limit of $\sim 665 \text{ mV}$ for this solar cell structure. The low IQE level in the short wavelength range is rather caused by a parasitic absorption

within the SiN_x antireflection coating. Unfortunately, this layer features a refractive index of ~2.2 and thus also an increased absorption, since it was not optimized to the low deposition temperature of *a*-Si:H yet. However, it should be noted that the additional absorption within the SiN_x does not alter the observed trend, that thicker *a*-Si:H layers lead to an increased *IQE*. As solar cells featuring the thickest *a*-Si:H layers also feature the thickest SiN_x this effect would be even increased.

5 CONCLUSIONS

p⁺nn⁺ solar cells were fabricated, where the diffused boron emitters on the front were passivated by *a*-Si:H of different thicknesses between 5 and 21 nm. A maximum efficiency of 17.8% was achieved for *a*-Si:H thickness of 15 nm, with an open-circuit voltage V_{OC} of 641 mV. The V_{OC} showed no dependence on the *a*-Si:H thickness, which was expected to decrease below an *a*-Si:H thickness of about 10 nm due to a decreased passivation quality found on lifetime samples. The measured internal quantum efficiency *IQE* of these cells increases in the short wavelength range with increasing *a*-Si:H thickness, although the V_{OC} was independent the *a*-Si:H thickness. Since *a*-Si:H shows a strong absorption within the short wavelength range, a decrease of the *IQE* was expected within that wavelength range. Further work is necessary for an understanding of those effects.

Analogous fabricated reference *p⁺nn⁺* solar cells passivated by Al₂O₃ achieved efficiency of up to 19% with the simple cell structure featuring only a phosphorous back surface field. That efficiency is more than 1% above the *a*-Si:H passivated cells, which demonstrates the superior passivation quality of Al₂O₃ on highly doped boron surfaces.

6 ACKNOWLEDGEMENTS

The authors would like to thank I. Druschke, A. Leimenstoll, F. Schätzle, D. Schmidt, S. Seitz for processing, E. Schäffer for measurements and M. Bivour for valuable discussions. This work was funded by the German Federal Ministry for the Environment, Nature Conservation and Nuclear Safety under contract number 0329849A (Th-ETA).

REFERENCES

- [1] D. Macdonald and L. J. Geerligs, Applied Physics Letters 85 (2004) 4061.
- [2] S. W. Glunz, S. Rein, J. Y. Lee, and W. Warta, Journal of Applied Physics 90 (2001) 2397.
- [3] P. P. Altermatt, H. Plagwitz, R. Bock, J. Schmidt, R. Brendel, M. J. Kerr, and A. Cuevas, in Proceedings of the 21st European Photovoltaic Solar Energy Conference, Dresden, Germany, 2006, p. 647.
- [4] J. Benick, B. Hoex, M. C. M. van de Sanden, W. M. M. Kessels, O. Schultz, and S. W. Glunz Applied Physics Letters 92 (2008) 253504/1.
- [5] B. Hoex, J. Schmidt, R. Bock, P. P. Altermatt, M. C. M. van de Sanden, and W. M. M. Kessels, Applied Physics Letters 91 (2007) 112107/1.
- [6] S. Dauwe, J. Schmidt, and R. Hezel, in Proceedings of the 29th IEEE Photovoltaics Specialists Conference, New Orleans, Louisiana, USA, 2002, p. 1246.
- [7] H. Plagwitz, M. Nerding, N. Ott, H. P. Strunk, and R. Brendel, Progress in Photovoltaics: Research and Applications 12 (2004) 47.
- [8] H. Plagwitz, Y. Takahashi, B. Terheiden, and R. Brendel, in Proceedings of the 21st European Photovoltaic Solar Energy Conference, Dresden, Germany, 2006.
- [9] R. A. Sinton and A. Cuevas, Applied Physics Letters 69 (1996) 2510.
- [10] A. Richter, J. Benick, and S. W. Glunz, in Proceedings of the 23rd European Photovoltaic Solar Energy Conference, Valencia, Spain, 2008, p. in print.
- [11] R. Brendel, in Proceedings of the 12th European Photovoltaic Solar Energy Conference (R. Hill, W. Palz, and P. Helm, eds.), H.S. Stephens & Associates, Bedford, UK, 1994, Amsterdam, The Netherlands, 1994, p. 1339.
- [12] D. Pysch, M. Bivour, K. Zimmermann, C. Schetter, M. Hermle, and S. W. Glunz in the proceedings of this conference, 2009.
- [13] D. A. Clugston and P. A. Basore, in Proceedings of the 26th IEEE Photovoltaic Specialists Conference, IEEE; New York, NY, USA, Anaheim, California, USA, 1997, p. 207.